

Proton-irradiation-induced anomaly in the electrical conductivity of a hydrogen-bonded ferroelastic system

Se-Hun Kim,^{1,2} Kyu Won Lee,¹ Kwang-Sei Lee,³ and Cheol Eui Lee^{1,*}¹*Department of Physics and Institute for Nano Science, Korea University, Seoul 136-713, Korea*²*Faculty of Science Education, Jeju National University, Jeju 690-756, Korea*³*Department of Nano Systems Engineering, Center for Nano Manufacturing, Inje University, Gimhae 621-749, Gyeongnam, Korea*

(Received 21 April 2009; revised manuscript received 6 August 2009; published 3 November 2009)

An anomalous abrupt drop in the electrical conductivity has been observed at the ferroelastic phase transition of a proton-irradiated system of hydrogen-bonded TiH_2PO_4 . As a result of the high-resolution ^{31}P NMR chemical-shift measurements, distinct changes in the atomic displacements due to the irradiation were identified in the ferroelastic and paraelastic phases. Besides, ^1H NMR spin-spin relaxation measurements revealed a change due to the irradiation in the proton dynamics at the ferroelastic phase transition, apparently accounting for the much-reduced electrical conductivity in the paraelastic phase of the irradiated system.

DOI: [10.1103/PhysRevB.80.172101](https://doi.org/10.1103/PhysRevB.80.172101)

PACS number(s): 76.60.-k, 61.80.Lj, 77.90.+k

Considerable attention has been paid to the KH_2PO_4 (KDP)-type crystals for their ferroelastic as well as (anti)ferroelectric phase transitions.^{1,2} The hydrogen-bonded KDP-type crystals are known to undergo structural phase transitions of a weak first order. Proton transport gives rise to ionic conduction and dielectric relaxation in these systems,³⁻⁶ whose electrical and elastic properties associated with the phase transitions have been studied in terms of domain-wall motions.^{7,8}

In contrast to the simultaneous ferroelectric and ferroelastic transitions in KDP, TiH_2PO_4 (TDP) undergoes antiferroelectric and ferroelastic phase transitions at well-separated temperatures, i.e., at $T_c=230$ K and $T'_c=357$ K, respectively.^{9,10} We have recently identified a peculiar mixed-phase boundary temperature T_s in TDP from temperature-dependent impedance spectroscopy.^{11,12} Distinct electrical responses were obtained below and above a Curie-Weiss temperature T_s , well above T_c . The polarization exhibited a paraelectric response above T_s and an antiferroelectric response below that temperature.^{11,12}

Two distinct domain structures are known in TiH_2PO_4 and TiH_2AsO_4 , i.e., the (001)/(100) domain structure disappearing above the ferroelastic phase and the (201) domain structure persisting above the ferroelastic phase transition.¹³ Elastic frustrations can take place in the ferroelastic phase in the interface regions between the domains due to random stress-strain relationships.¹

There are three different crystallographic hydrogen bonds with inequivalent H sites in TDP according to x-ray and neutron-scattering measurements.¹⁴ Two shorter bonds of length 0.243 and 0.245 nm are centrosymmetric forming zig-zag chains along the c axis. The protons are at special positions of a center of inversion undergoing an order-disorder transition.¹⁵ The longest bond of length 0.25 nm is asymmetric along the b axis, with the protons at a general position being ordered at all temperatures. The very short hydrogen bonds and the very heavy Ti^+ ion mass are peculiar to TDP, playing a vital role in the phase transitions.

The hydrogen-bonded antiferroelectrics are relatively less understood than the KDP-type crystals undergoing a ferroelectric transition, the textbook antiferroelectric $\text{NH}_4\text{H}_2\text{PO}_4$ being an exception.^{15,16} The antiferroelectric transition is

known to be associated with lattice strain and antiferroelectric phases have been reported in some ferroelectrics under external pressure.¹⁷ The effect of local ferroelastic strain on the proton ordering has been reported in squaric acid, in which the protons are antiferroelectrically ordered below T_c with simultaneous distortion of the squarate units.¹⁸ Coexistence of order-disorder and displacive behaviors in the ferroelectrics have been found¹⁹⁻²¹ under co-occurrence of (anti)ferroelectric and ferroelastic transitions. Continuous chemical shifts of nuclear-magnetic-resonance (NMR) peak positions arise from the displacive component in the structural phase transition involving proton order-disorder. Study of the coupling of proton ordering and ferroelastic shear strain at the phase transitions in TDP can be very interesting in view of the proton motion which in the proton-lattice coupling model is associated with the PO_4 tetrahedral motions.²² In this regard, we have carried out electrical conductivity as well as ^1H and ^{31}P NMR measurements in order to probe the charge dynamics and atomic displacements in view of the antiferroelectricity and ferroelasticity in TDP.

Polycrystalline bulks of TDP, with and without irradiation with a 1 MeV proton beam of spot radius 0.5 cm at a dose of $10^{15}/\text{cm}^2$, were pulverized and pelletized into a disk of diameter of 13 mm and thickness 0.78 mm. Gold electrodes were put on the flat faces of the disks for electrical conductivity measurements from the complex impedance in a frequency range from 10 to 2 MHz by using a Quadtech 7600 impedance analyzer. The NMR measurements were made by using a 400 MHz pulsed BRUKER DSX 400 NMR spectrometer between 200 and 400 K. High-resolution ^{31}P magic angle spinning NMR measurements were carried out employing a Larmor frequency of 243 MHz with a spinning frequency of 7 kHz. The chemical-shift measurements were made relative to a solution of H_3PO_4 , a ^{31}P standard. The ^1H NMR spin-spin relaxation was measured by the conventional solid echo pulse sequence, $(\pi/2)_{0^\circ} - \tau - (\pi/2)_{90^\circ}$. The change in the number by the proton irradiation of $10^{15}/\text{cm}^2$, corresponding only to one in 10^7 lattice sites, may give rise to no significant change in the ^1H NMR intensities or in the crystal composition.

The real and imaginary parts of the complex impedance of the TDP system before and after the proton irradiation

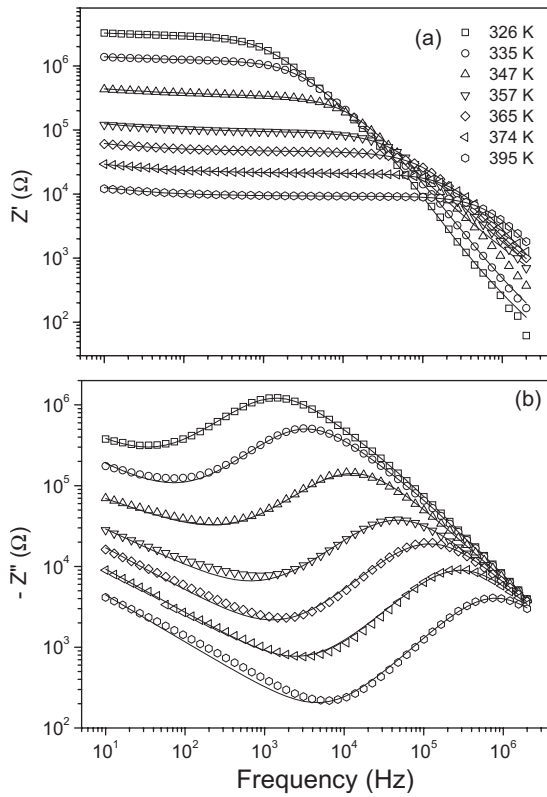


FIG. 1. (a) Real and (b) imaginary parts of the complex impedance of the TDP system before the proton irradiation as functions of frequency and temperature.

were obtained as functions of frequency and temperature (Figs. 1 and 2). Figure 3 shows the temperature dependence of the dc electrical conductivity before and after the proton-beam irradiation, obtained from the impedance measurements by using the relation $\sigma(\omega) = \omega \epsilon_o \epsilon''$, ϵ'' being the imaginary part of the complex impedance. The dispersion of the electrical conductivity in disordered solids is generally described by the Jonscher's relation, $\sigma(\omega) = \sigma_o + A\omega^n$, where σ_o is the dc conductivity of the sample and the power-law exponent n ($0 < n < 1$) represents the degree of interaction between the mobile ions and their environment. While the dc electrical conductivity σ_o , which is the long-term response to the electric field,²³ mostly showed a monotonic increase with temperature before the proton irradiation, an anomalous drop is manifest at the ferroelastic transition temperature after the irradiation (Fig. 3). It is to be noted that whereas the electrical conductivity shows a noticeable change in the ferroelastic phase only near T'_c , a drastic and marked change arises from the proton irradiation in the paraelastic phase above T'_c .^{20,24} It is to be noted that as expected the activation energies obtained from the straight-line portion of the conductivity in Fig. 3 are in excellent agreement with the rotating-frame spin-lattice relaxation-time ($T_{1\rho}$) measurements reported in our previous work.²⁴ The temperature dependence of the coefficient A is shown in Fig. 4 in order to provide information on the relative sizes of the dc and ac responses.

In order to study the changes in the microscopic lattice environments arising from proton irradiation, high-resolution ³¹P NMR chemical-shift measurements were made for prob-

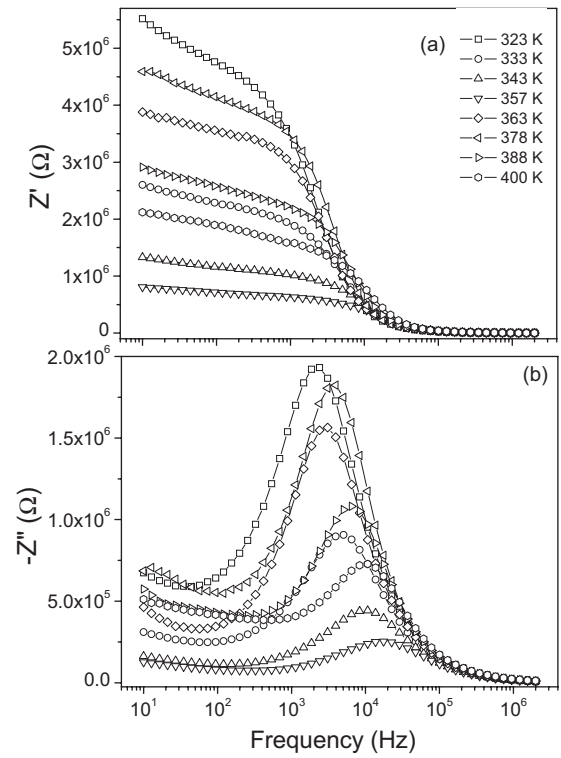


FIG. 2. (a) Real and (b) imaginary parts of the complex impedance of the TDP system after the proton irradiation as functions of frequency and temperature.

ing phosphorous atomic displacements in the PO_4 tetrahedra. Figure 5 shows the temperature dependence of the change, $\Delta\sigma_{iso}$, in the ³¹P NMR isotropic chemical shift due to the proton irradiation. It is quite interesting to note the fact that the ferroelastic phase transition in TDP is marked by a

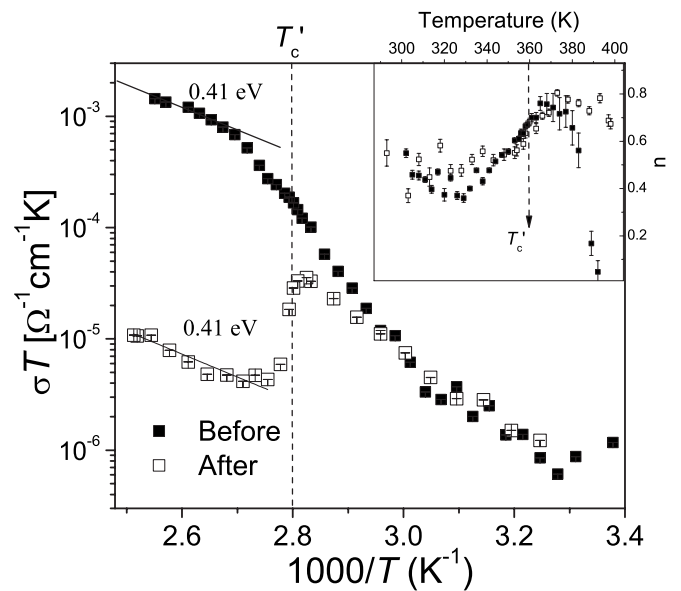


FIG. 3. Temperature dependence of the dc electrical conductivity in TDP before and after the proton-beam irradiation. Inset: the power-law exponent n of the frequency dependence as a function of temperature.

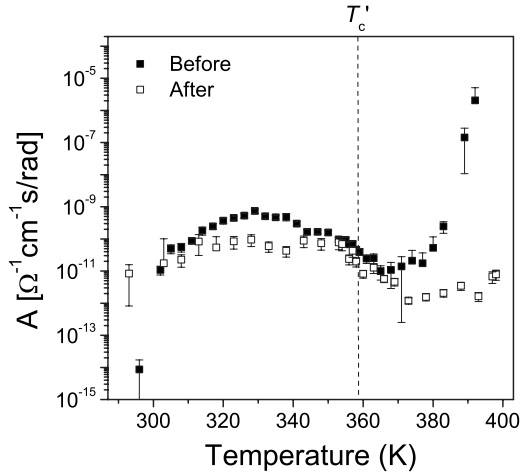


FIG. 4. Temperature dependence of the coefficient A in the Joncher's relation before and after the proton-beam irradiation.

change in $\Delta\sigma_{iso}$. The isotropic chemical shift following the proton irradiation moved in the opposite directions below and above T'_c . The isotropic chemical shift below the ferroelastic phase-transition temperature T'_c in the proton-irradiated TDP moved toward low frequencies by about $\Delta\sigma_{iso}=16$ Hz (Refs. 25 and 26) whereas it moved toward high frequencies above T'_c . Thus, quite distinct changes in the electron charge distribution and thus those in the lattice strain are detected in the ferroelastic and paraelastic phases by the high-resolution NMR techniques employed in this work.

The ^1H NMR spin-spin relaxation rate (T_{2E}^{-1}) data were well fitted by a double exponential form at all temperatures, giving two decay constants corresponding to the sharp and broad lines in the ^1H NMR line shape. The short-term decay reflects atomic diffusion among the "rigid-lattice" protons corresponding to the broad Gaussian ^1H NMR line-shape component whereas the long-term decay is ascribed to the mobile protons corresponding to the narrow Lorentzian component.²⁷ Figure 6 shows the temperature dependence of

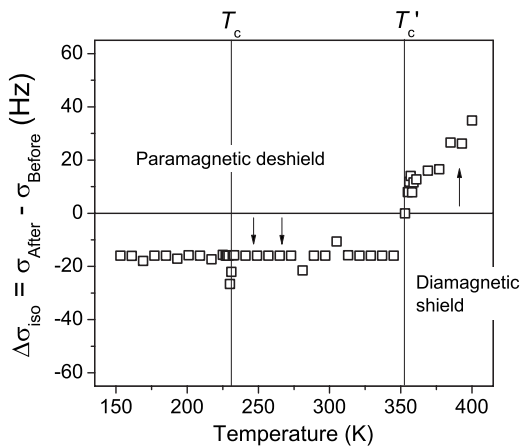


FIG. 5. Temperature dependence of the change, $\Delta\sigma_{iso}$, in the ^{31}P NMR isotropic chemical shift due to the proton irradiation. T'_c indicates the ferroelastic phase-transition temperature. The errors are within the size of the symbols.

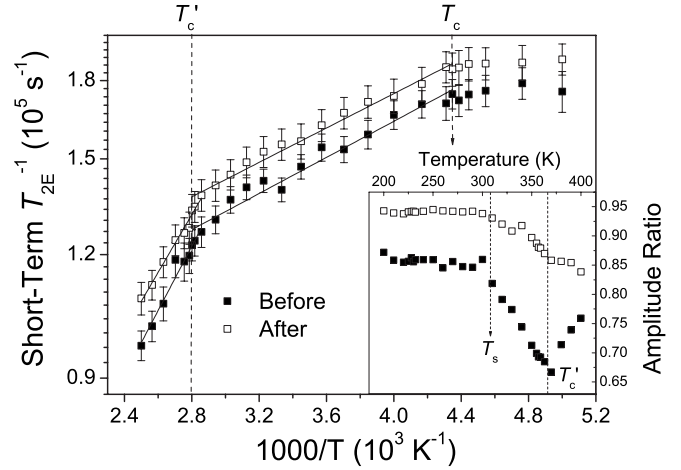


FIG. 6. Temperature dependence of the short-term exponential decay rate obtained from the ^1H NMR spin-spin relaxation measurements in TDP before and after the proton-beam irradiation. The inset shows the amplitude fraction of the short-term decay component.

the short-term spin-spin relaxation rate.

The spin-spin relaxation rate for the lattice diffusion of the Arrhenius type is related to the diffusion coefficient D by

$$1/T_2 \propto D^{-1} = D_o^{-1} e^{+\Delta E/kT}, \quad (1)$$

where ΔE is the activation energy or a potential barrier of diffusion.²⁸ While the short-term decay constant shows little change in the antiferroelectric phase, an overall decrease with increasing temperature is noticed above T_c , indicative of the rigid-lattice protons undergoing lattice diffusion whose activation energies may be obtained from the slopes in Fig. 6. Before and after the irradiation, activation energies of 18 and 17 meV were obtained in the ferroelastic phase

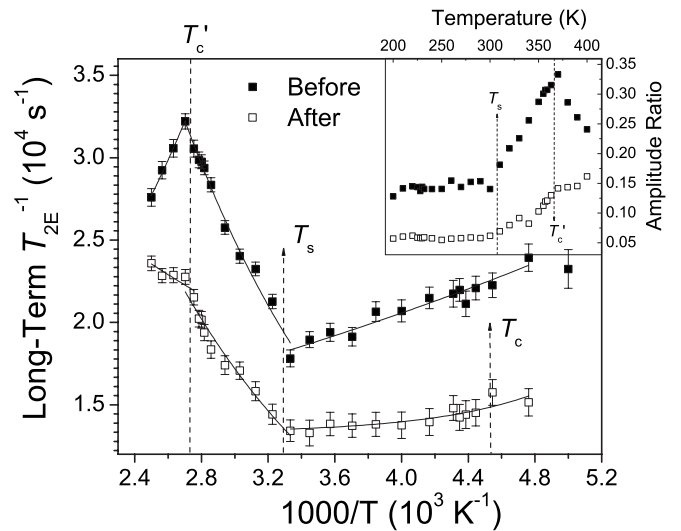


FIG. 7. Temperature dependence of the long-term spin-spin relaxation rate obtained from the ^1H NMR spin-spin relaxation measurements in TDP before and after the proton-beam irradiation. The inset shows the amplitude fraction of the long-term decay component.

whereas those of 64 and 57 meV were obtained in the paraelastic phase T'_c , respectively.¹⁸

Three distinct regimes of random motions of the Arrhenius type, with a correlation time τ , are manifest in the temperature-dependent long-term spin-spin relaxation rate (Fig. 7). The spin-spin relaxation rate is given by $T_2^{-1} \propto \tau_o^{-1} \exp[+E_a/k_B T]$ in the fast motion regime ($\omega\tau \ll 1$),²⁸ where ω is the Larmor frequency and E_a is the activation energy, which can be obtained from the slopes in Fig. 7. Distinct activation energies and motional limits before and after the proton irradiation may thus be obtained in the three distinct temperature ranges separated by $T_s \approx 305$ K and T'_c (Fig. 7).^{11,27} It is of particular interest to note the change in the proton motional limits in the paraelastic phase ($T > T'_c$) due to the proton-beam irradiation. The proton-beam treatment gives rise to a slow dynamics of the hydrogen motion in the paraelastic phase of the TDP system. Thus, the abrupt drop in the electrical conductivity at T'_c in the proton-irradiated TDP may well be explained by an abrupt change in the mobility. In the same context, it is worth noting the increase in the population of the rigid-lattice protons following the proton-beam irradiation (see insets of Figs. 6 and 7). The increase in the population of the “rigid-lattice protons” in the system exposed to the proton beam may also be understood in terms of the surplus protons, generated by irradiation, decreasing the number of lattice sites accessible to diffusing

protons, effectively decreasing the relative number of “mobile” protons.

In summary, we have investigated the proton-irradiation effects on the electrical conductivity of the hydrogen-bonded system of TiH_2PO_4 undergoing well-separated antiferroelectric and ferroelastic phase transitions. As a result, an anomalous, abrupt drop in the electrical conductivity was found at the ferroelastic phase transition of the proton-irradiated system, and possible clues were sought by means of the high-resolution ^{31}P NMR chemical shift and ^1H NMR spin-spin relaxation measurements. Thus, distinct phosphorous atomic displacements of the PO_4 tetrahedra in the ferroelastic and paraelastic phases of the proton-irradiated system were identified. A motional slowing down of proton dynamics in the paraelectric phase of the proton-irradiated system was revealed as well, possibly explaining the origin of the marked decrease in the electrical conductivity.

This work was supported by the Korea Ministry of Education, Science and Technology (NRL Program R0A-2008-000-20066-0, User Program of Proton Engineering Frontier Project, KRF-2007-314-C00129). We thank H.-J. Woo at the Korea Institute of Geoscience and Mineral Resources (KIGAM) for the proton-beam irradiation, and the measurements at the Korean Basic Science Institute (KBSI) are acknowledged.

*Corresponding author; rscel@korea.ac.kr

¹E. K. H. Salje, *Phase Transitions in Ferroelastic and Co-elastic Crystals* (Cambridge University Press, Cambridge, England, 1992); C. E. Lee, C. H. Lee, J. H. Kim, and K. S. Lee, *Phys. Rev. Lett.* **75**, 3309 (1995).

²A. V. Hippel, *Dielectrics and Waves* (Wiley, New York, 1966); C. H. Lee, K. W. Lee, C. E. Lee, and K. S. Lee, *Phys. Rev. B* **55**, 11088 (1997).

³J. Dolinšek, M. Karayanni, and G. Papavassiliou, *Solid State Ionics* **125**, 159 (1999).

⁴V. H. Schmidt and E. A. Uehling, *Phys. Rev.* **126**, 447 (1962).

⁵J. E. Diosa, R. A. Vargas, I. Albinsson, and B.-E. Mellander, *Phys. Status Solidi B* **241**, 1369 (2004).

⁶Y. Matsuo, J. Hatori, Y. Nakashima, and S. Ikehata, *Solid State Commun.* **130**, 269 (2004).

⁷Y. N. Huang, X. Li, Y. Ding, Y. N. Wang, H. M. Shen, Z. F. Zhang, C. S. Fang, S. H. Zhuo, and P. C. W. Fung, *Phys. Rev. B* **55**, 16159 (1997).

⁸Y. N. Huang, Y. N. Wang, and H. M. Shen, *Phys. Rev. B* **46**, 3290 (1992).

⁹K. W. Lee, D. K. Oh, C. E. Lee, J. K. Kang, C. H. Lee, and J. Kim, *J. Chem. Phys.* **117**, 8004 (2002).

¹⁰R. Blinc and B. Zeks, *Ferroelectrics* **72**, 193 (1987).

¹¹S. H. Kim, K. W. Lee, C. E. Lee, K.-S. Lee, D. H. Kim, and D. Y. Jang, *Appl. Phys. Lett.* **89**, 102901 (2006).

¹²S. H. Kim, K. W. Lee, B. H. Oh, and C. E. Lee, *Phys. Rev. B* **76**, 172104 (2007).

¹³K. Irokawa, M. Komukae, T. Osaka, and Y. Makita, *J. Phys. Soc. Jpn.* **63**, 1162 (1994).

¹⁴R. J. Nelmes and R. N. P. Choudhary, *Solid State Commun.* **38**,

321 (1981).

¹⁵J. Seliger, V. Zagar, R. Blinc, and V. H. Schmidt, *J. Chem. Phys.* **88**, 3260 (1988); I.-H. Oh, J. J. Kweon, and B. H. Oh, and C. E. Lee, *J. Korean Phys. Soc.* **53**, 3497 (2008).

¹⁶M. E. Lines and A. M. Glass, *Principles and Applications of Ferroelectrics and Related Materials* (Oxford University Press, New York, 1982); Y. Kim, S.-I. Kwun, S. Park, B. Oh, and D. Lee, *Phys. Rev. B* **28**, 3922 (1983).

¹⁷K. Deguchi, S. Azuma, Y. Kobayashi, S. Endo, and M. Tokunaga, *Phys. Rev. B* **69**, 024106 (2004).

¹⁸D. T. Vigen, *Phys. Rev. B* **25**, 4804 (1982).

¹⁹N. Dalal, A. Klymchyov, and A. Bussmann-Holder, *Phys. Rev. Lett.* **81**, 5924 (1998).

²⁰A. Bussmann-Holder, N. Dalal, R. Fu, and R. Migoni, *J. Phys.: Condens. Matter* **13**, L231 (2001).

²¹R. Blinc, *Ferroelectrics* **301**, 3 (2004).

²²A. Bussmann-Holder and K. H. Michel, *Phys. Rev. Lett.* **80**, 2173 (1998).

²³N. Chabchoub and H. Khemakhem, *J. Alloys Compd.* **370**, 8 (2004).

²⁴S. H. Kim, K. W. Lee, J. W. Jang, C. E. Lee, J. Y. Choi, K. S. Lee, and J. Kim, *Phys. Rev. B* **72**, 214107 (2005).

²⁵S. J. van Reeuwijk, A. Puig-Molina, and H. Graafsma, *Phys. Rev. B* **62**, 6192 (2000).

²⁶S. J. van Reeuwijk, A. Puig-Molina, and H. Graafsma, *Phys. Rev. B* **64**, 134105 (2001).

²⁷S.-H. Kim, K. W. Lee, J. H. Han, and C. E. Lee, *Solid State Commun.* **144**, 1 (2007).

²⁸C. P. Poole and H. A. Farach, *Relaxation in Magnetic Resonance* (Academic, New York, 1971).